PHYSICAL REVIEW E **86**, 020601(R) (2012)

# Imbibition of a textured surface decorated by short pillars with rounded edges

Noriko Obara and Ko Okumura*

*Department of Physics, Graduate School of Ochanomizu University, 2-1-1, Otsuka, Bunkyo-ku, Tokyo 112-8610, Japan*

(Received 8 July 2011; revised manuscript received 31 May 2012; published 1 August 2012)

Imbibition of micropatterned surfaces can have broad technological and fundamental implications for areas ranging from biomedical devices and fuel transport to writing with ink. Despite rapidly growing interests aimed at various applications, a fundamental physical understanding of the imbibition dynamics is still in its infancy. Recently, two simple scaling regimes for the dynamics have been established for a textured surface decorated with long pillars whose top and bottom edges are sharp. Here, we study the imbibition dynamics of textured surfaces decorated by short pillars with rounded edges, to find a different scaling regime. Interestingly, this regime originates not from the balance of two effects but from the hybrid balance of three effects. Furthermore, this scaling law can be universal or independent of the details of the texture geometry. We envision that this potentially universal scaling regime might be ubiquitous and will be useful in the handling and transportation of a small amount of liquid.

DOI: 10.1103/PhysRevE.86.020601 PACS number(s): 68.03.Cd, 47.61.−k, 89.75.Da

Micropatterned surfaces have been actively studied for many applications, such as wetting [1–3], liquid-drop transportation [4–6], and microfluidics applications [7,8] essential in biology, medicine, and chemistry [9]. Among these various possibilities, interest in the imbibition of textured surfaces [10,11] has grown rapidly from different viewpoints, from a fundamental understanding of scaling regimes [12], of writing with ink [13], and of the penetration of a solid into nanopillar arrays [14], to practical methods for obtaining bioinspired self-repairing slippery surfaces [15,16], controlled and patterned film coating [17–19], and paper-based microfluidics that is promising for diagnostic devices for the developing world and in environmental monitoring [20]. Despite these increasing interests, a fundamental physical understanding of the scaling regimes of the imbibition phenomena is very limited, as described below.

The classic example of imbibition is capillary rise [21]. The viscous regime is well described by the Washburn theory. In this regime, the capillary drive is balanced by a viscous drag due to the Poiseuille flow inside a capillary tube. As a result, the imbibition length $x$ scales as the square root of elapsed time $t$ ($x \sim t^{1/2}$). This law seems applicable to the imbibition of porous media. However, a detailed physical understanding is lacking. In fact, many other scaling exponents have been found for porous media without any physical interpretations [22–24].

Recently, a detailed understanding of the scaling laws for imbibition in porous materials has been obtained by using a textured surface decorated by long pillars with sharp edges (top and bottom edges of pillars are sharp) as a model of porous materials [12]. Two scaling regimes are identified for the imbibition dynamics. Both regimes are governed by the balance between the capillary drive and the viscous drag, which leads to the Washburn dynamics ($x \sim t^{1/2}$). Both regimes are distinguished by the nature of viscous drag: one due to the Poiseuille drag on the substrate and the other one due to the drag on the lateral surfaces of pillars. This physical picture was confirmed by the agreement between theory and experimental data for the dynamics [12], under the assumption that the thickness of the film imbibing the texture is comparable to pillar heights. This assumption is established from a different static viewpoint in Ref. [25]. A theoretical consideration [26] further clarifies that this assumption is valid only when the pillars are long and have sharp edges.

We fabricated textured surfaces decorated by short pillars with rounded edges instead of sharp edges. As a result, we find different scaling laws where the imbibition length $x$ scales as one-third power of elapsed time $t$ ($x \sim t^{1/3}$). This striking difference comes from the fact that the film thickness is no longer a constant (or not equal to the pillar height). In fact, the film thins down as imbibition proceeds.

Intriguingly, the imbibition dynamics found here is governed by the hybrid balance of three effects: capillary drive, and viscous and gravitational drags. In addition, this scaling law is independent of the details of the texture: The scaling can be quite universal and might explain many other imbibition phenomena and will be useful in various microfluidic applications, for example, in biomedical devices [20].

We fabricated a textured surface with micron scale features on a square plate of centimeter size, as shown in Figs. 1(a)–1(c), thanks to a recently proposed method [27]. In this simple method, a laser printer is used to generate a toner pattern. Then, the pattern is thermally transferred to a metal substrate to serve as a mask for etching. We used an etched copper substrate in our experiment. We analyzed the resulting surface by using a microscope VHX-1000 (Keyence) and obtained an average profile as in Fig. 1(d). We see that the texture is formed as short pillars with rounded edges: The radii of the curvature at the top and bottom edges are rather large and are not well separated from the other texture scales.

Once the end of a textured surface touches the horizontal surface of a liquid bath of silicone oil, the imbibition can be imaged as in Figs. 1(e) and 1(f). The tilt angle $\theta$ of the textured surface governs an effective gravity constant $G$ along the direction of penetration:

$$G = g \sin\theta, \tag{1}$$

where $g$ is 9.8 m/s$^2$.

*The corresponding author's e-mail address is okumura@phys.ocha.ac.jp

 

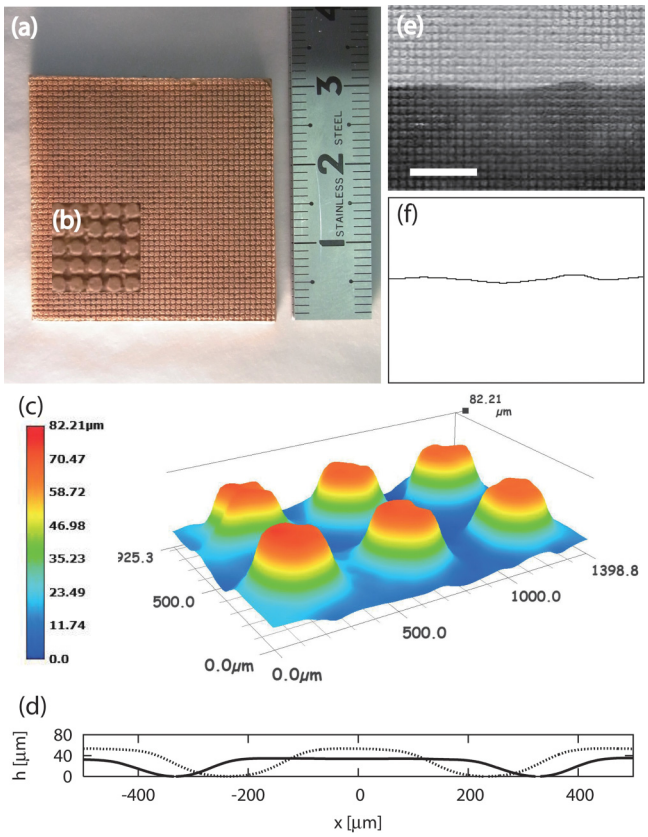


FIG. 1. (Color online) (a) and (b) Overview and magnified view, respectively, of a textured surface, denoted A below. (c) Magnified overview of a textured surface, denoted B below. (d) Average section of the textured surface A (solid line) and B (dashed line). (e) Liquid film penetrating on substrate A; the darker part is the region invaded by the liquid and the white bar corresponds to 5 mm. (f) Binary image of the front line obtained from (e). The imbibition length $x$ is determined as an average height of this front line.

In order to determine the position $x$ of the imbibing front, we took several images per minutes by a digital camera (Ricoh CX2). After obtaining a binary image as in Fig. 1(f), we followed the front-line shape with time and calculated the average height at each time by using MATHEMATICA. When liquid starts to imbibe the surface, a meniscus is formed at the bottom of the film just above the bath surface. The imbibition length $x$ is measured from the top of this meniscus.

The results obtained from sample A are shown in Figs. 2(a) and 2(b), where the kinematic viscosities $\eta/\rho$ and the angles $\theta$ are indicated for each series of data. Here, $\rho$ is the density of the oil. The error bars for Figs. 2(a) and 2(b) are smaller than the size of the symbols.

In Figs. 2(a) and 1(b), we see that both viscosity and gravity slow down the dynamics. We thus need a theory where the capillarity is opposed by viscosity and gravity: The three terms in the Navier-Stokes equation should compete.

To develop such a model, we consider the limit where the penetrating film is thin. In such a case the equation for velocity $V$ in the $x$ direction reduces to the lubrication equation [21]

$$\frac{\partial p}{\partial x} - \rho G = \eta \nabla^2 V, \tag{2}$$

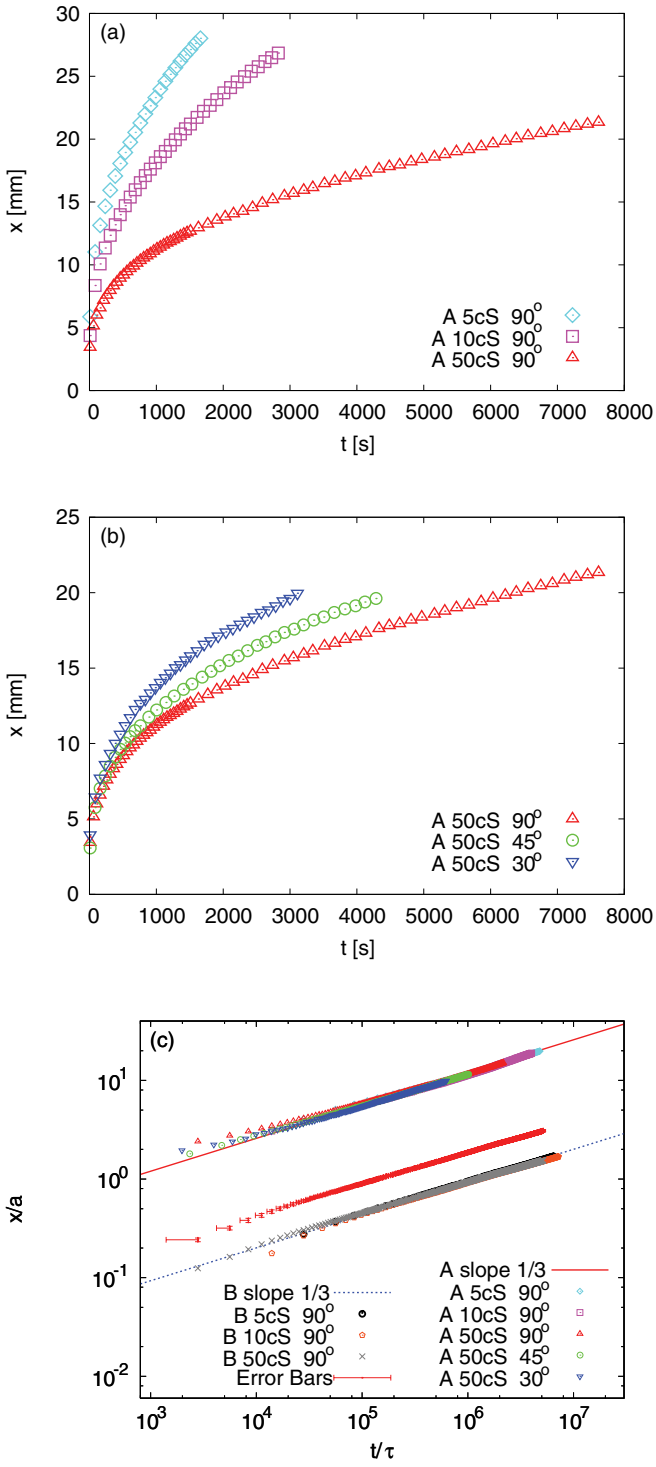


FIG. 2. (Color online) (a) and (b) Effect of viscosity and of gravity, respectively, on the imbibition length $x$ as a function of time $t$ obtained from surface A. (c) Collapse of the data in (a) and (b) as a result of rescaling based on Eq. (8), together with another collapse of the data obtained from surface B and with yet another data set for demonstrating error bars.

where the pressure can be expressed as $p = p_0 + \gamma C$ by taking into account the Laplace pressure jump at the interface [21]. Here, we have denoted the atmospheric pressure, the surface

tension of the liquid, and the curvature of the liquid-air interface as $p_0$, $\gamma$, and $C$, respectively.

Since our data suggest that viscosity and gravity are equally important, we compare $\rho G$ and $\partial p/\partial x$ ($\simeq \gamma C/x$) in Eq. (2) to obtain an estimation of the local curvature at the imbibition front:

$$C \simeq \rho G x/\gamma. \tag{3}$$

In other words, $\rho G$ and $\gamma C/x$ in Eq. (2) are assumed to be of the same order. Thus, we obtain

$$\rho G \simeq \eta \nabla^2 V \quad \text{or} \quad \gamma C/x \simeq \eta \nabla^2 V, \tag{4}$$

together with Eq. (3).

Both the first and second equations in Eq. (4) result in the same equation,

$$x = \alpha t^{1/3}, \tag{5}$$

at the level of scaling law (note that $V = dx/dt$), with

$$\alpha \simeq \left(\frac{\gamma^2}{\rho G \eta}\right)^{1/3}. \tag{6}$$

Here, we have assumed that the Laplacian in Eq. (4) scales as $C^2$, i.e.,

$$|\nabla^2| \simeq C^2. \tag{7}$$

The physical meaning of this assumption (justified below) is to set, at the imbibing front, the film thickness $|\nabla|^{-1}$ to a characteristic length set by the curvature $C^{-1}$. From Eq. (3), this means that the film thickness scales as $1/x$, and thus decreases as $x$ increases. To understand this, we recall the role of $\nabla^2$ in Eq. (2): The (smallest) viscous length scale $|\nabla|^{-1}$ represents the thickness of the film near the front inside which the Poiseuille flow develops and velocity varies from 0 to $V$.

By introducing the capillary length $a$ of the order of 1 mm by $a^2 = \gamma/(\rho G)$, Eq. (5) is renormalized as

$$x/a \simeq (t/\tau)^{1/3}, \tag{8}$$

where the characteristic time scale $\tau$ is defined as $\tau = \eta a/\gamma$, which is of the order of a few ms or less.

To show a good agreement of this model with experiments, in Fig. 2(c) we collect the five series of data with different viscosities $\eta$ and different tilt angles $\theta$ [shown in Figs. 2(a) and 2(b)] on the same plot with the renormalization of both axes specified by Eq. (8). As the model predicts, all the data from surface A collapse quite well onto a line with a slope of one-third power. As shown in the same plot, the data from surface B collapse well. The collapsed data from surface B are shifted downwards by a factor of 10 to avoid overlap with the data from surface A [28].

The error bars in Fig. 2(c) are very small. For example, the data set labeled "B 10 cS 90°" are shown with error bars in Fig. 2(c) (with a shift to avoid overlap). The errors in the vertical axis are always smaller than the size of the symbols and those in the horizontal time axis are visible only at very early times ($t/\tau \lesssim 10^{-4}$).

The good agreement between the theory and the experimental data supports our assumptions, i.e., Eqs. (3) and (7). We further justify these assumption by visualizing the film thickness (see Fig. 3). For the visualization, we used a commercial solution (TA434ED-0, TASCO) for gas-leak detection.

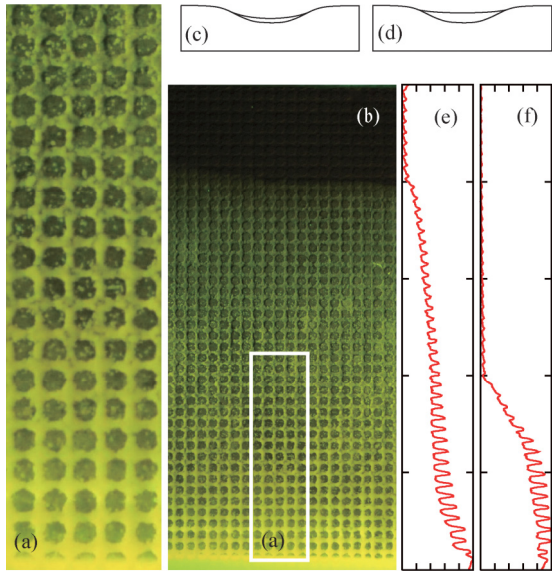


FIG. 3. (Color online) (a) Magnified view of the penetrating liquid film on surface A, visualized by using fluorescence molecules and UV light. (b) Overview of the film. A part of (b) is magnified in (a). (c) and (d) Thin and thick films, respectively, on the surface; the thicker the film, the weaker the surface curvature. (e) Fluorescent intensity that reflects film thickness as a function of height obtained from (b). (f) The same plot as (e) but obtained at an earlier elapsed time.

This contains fluorescent molecules that emit green light when excited. We dissolved this chemical into olive oil and used this mixture for the imbibition experiment. We used a UV light source (UV-LED375-03SB, Southwalker) for the excitation and put a filter (SP 4, Fuji Film) in front of the light that cuts green light. We placed a bandpass filter (BPB 55, Fuji Film) that selectively passes green light in front of a digital camera (D700, Nikon).

From the global view given in Fig. 3(b), in contrast to the assumption made in the previous experiments [12,17], we see that the film thickness thins down with height. From the magnified view in Fig. 3(a), we see that at the bottom the film surface is nearly flat while at the top the surface nearly follows the curvature of the texture: The film thins down and the curvature increases as the height increases, as illustrated in Figs. 3(c) and 3(d). This is consistent with the physical meanings of the assumption in Eqs. (3) and (7): Near the imbibing front, the curvature of the film surface is consistent to scale as $x$ and the film thickness to scale as the inverse of $x$.

Quantitative results are shown in Figs. 3(e) and 3(f), where the intensity (horizontal axis) is plotted as a function of height (vertical axis). Figure 3(e) shows the profile for Fig. 3(b) while Fig. 3(f) shows a profile at an earlier time, or at a smaller imbibition height. These two profiles confirm that the film thickness near the front (but several pillars away from the real front) gets smaller as imbibition proceeds, as the assumption in Eq. (7) suggests.

The image analysis in Figs. 3(e) and 3(f) was done by creating macro codes for IMAGE J. Note that the intensity shown here should be a monotonic increasing function of the film thickness (the brighter, the thicker). However, the intensity may not be simply proportional to the film thickness.

The role of the pillars is clarified by the visualization [see Figs. 3(c) and 3(d)]: It is (1) to provide curvature for the pressure drop, i.e., the driving force, at the imbibing front and (2) to limit the maximum thickness to the pillar height, allowing the lubrication approximation.

Equations (5) and (6) are independent of pillar height, space, and radius: The theory is independent of the detailed geometry of the substrate or the pillars. In other words, when the pillars are short and have rounded edges, at the propagating front, the radius of curvature $C^{-1}$ is determined by Eq. (2) as in Eq. (3) because this is the only natural local length scale available in the present case (the film thickness is no longer comparable to pillar height [26]).

The one-third power law for the imbibition dynamics has been discussed also in a different context of capillary rise into a sharp corner [29–31]. Such a sharp geometry is rather different from and nearly opposite to the rounded-edge geometry of our pillars. Accordingly, a striking difference appears in the smallest viscous scale: It is identified as the film thickness in our case, while it is as the wall distance along the liquid surface for a sharp corner.

In conclusion, we have shown that the imbibition of the textured surface formed by short pillars with rounded edges advances as $x \simeq t^{1/3}$ by keeping a hybrid balance of the capillary drive and viscous and gravitational drags. This dynamics is quite different from the recently established dynamics ($x \simeq t^{1/2}$) for surfaces comprising long pillars with sharp edges [12,17]. Surprisingly, the present one-third power law is universal in the sense that the scaling is independent of the geometry of the pillars forming the texture.

We point out that our scenario for the scaling dynamics is different from the standard one. Recently, a number of simple scaling laws have been found in the dynamics governed by the Navier-Stokes equation [21]: the breakup [32–35] and coalescence [36–42] of liquid drops, the dynamics of a thin liquid film [43–46], and so forth. Such recently found simple scaling laws most frequently result from the competition between two dominant terms in the equation. However, this should be only the simplest scenario. In fact, we find here a scaling dynamics resulting from a hybrid balance of more than two terms. Although there have been such examples, which include those in different contexts [47–49], our clear example of this unusual scenario, confirmed through the good agreement between experiment and theory, encourages us to consider other possibilities of simple dimensional analysis to explain unresolved scaling laws in the field.

The authors thank David Quéré and Etienne Reyssat for discussions on capillary rise in sharp corners, Masaki Sano for discussions on imbibition of papers, and Nicolas Vandewalle for useful comments. K.O. acknowledges MEXT, Japan.

[1] D. Quéré, Nat. Mater. **1**, 14 (2002).
[2] A. Tuteja, W. Choi, M. Ma, J. Mabry, S. Mazzella, G. Rutledge, G. McKinley, and R. Cohen, Science **318**, 1618 (2007).
[3] M. Liu, Y. Zheng, J. Zhai, and L. Jiang, Acc. Chem. Res. **43**, 368 (2009).
[4] K.-H. Chu, R. Xiao, and E. Wang, Nat. Mater. **9**, 413 (2010).
[5] N. A. Malvadkar, M. J. Hancock, K. Sekeroglu, W. J. Dressick, and M. C. Demirel, Nat. Mater. **9**, 1023 (2010).
[6] G. Lagubeau, M. Le Merrer, C. Clanet, and D. Quere, Nat. Phys. **7**, 395 (2011).
[7] H. Gau, S. Herminghaus, P. Lenz, and R. Lipowsky, Science **283**, 46 (1999).
[8] T. M. Squires and S. R. Quake, Rev. Mod. Phys. **77**, 977 (2005).
[9] A. G. Smart, Phys. Today **64**(4), 16 (2011).
[10] E. Washburn, Phys. Rev. **17**, 273 (1921).
[11] J. Bico, C. Tordeux, and D. Quéré, Europhys. Lett. **55**, 214 (2001).
[12] C. Ishino, M. Reyssat, E. Reyssat, K. Okumura, and D. Quéré, Europhys. Lett. **79**, 56005 (2007).
[13] J. Kim, M.-W. Moon, K.-R. Lee, L. Mahadevan, and H.-Y. Kim, Phys. Rev. Lett. **107**, 264501 (2011).
[14] P. Gaillard, Y. Saito, and O. Pierre-Louis, Phys. Rev. Lett. **106**, 195501 (2011).
[15] T. Wong, S. Kang, S. Tang, E. Smythe, B. Hatton, A. Grinthal, and J. Aizenberg, Nature (London) **477**, 443 (2011).
[16] A. Lafuma and D. Quéré, Europhys. Lett. **96**, 56001 (2011).
[17] L. Courbin, E. Denieul, E. Dressaire, M. Roper, A. Ajdari, and H. Stone, Nat. Mater. **6**, 661 (2007).
[18] M. Blow, H. Kusumaatmaja, and J. Yeomans, J. Phys.: Condens. Matter **21**, 464125 (2009).
[19] T. Ohzono, H. Monobe, K. Shiokawa, M. Fujiwara, and Y. Shimizu, Soft Matter **5**, 4658 (2009).
[20] A. Martinez, S. Phillips, and G. Whitesides, Proc. Natl. Acad. Sci. USA **105**, 19606 (2008).
[21] P.-G. de Gennes, F. Brochard-Wyart, and D. Quéré, *Gouttes, Bulles, Perles et Ondes*, 2nd ed. ( Belin, Paris, 2005).
[22] T. H. Kwon, A. E. Hopkins, and S. E. O'Donnell, Phys. Rev. E **54**, 685 (1996).
[23] A. S. Balankin, R. G. Paredes, O. Susarrey, D. Morales, and F. C. Vacio, Phys. Rev. Lett. **96**, 056101 (2006).
[24] A. M. Miranda, I. L. Menezes-Sobrinho, and M. S. Couto, Phys. Rev. Lett. **104**, 086101 (2010).
[25] N. Obara and K. Okumura, J. Phys. Soc. Jpn. Suppl. (to be published in September, 2012).
[26] M. Hamamoto-Kurosaki and K. Okumura, Eur. Phys. J. E **30**, 283 (2009).
[27] C. Easley, R. Benninger, J. Shaver, W. Steven Head, and D. Piston, Lab Chip **9**, 1119 (2009).
[28] The two collapsed lines from A and B also collapse with small errors, which suggests a possible weak dependence on contact angles or smaller-scale texture features of the dimensionless coefficient of Eq. (8).
[29] L.-H. Tang and Y. Tang, J. Phys. II France **4**, 881 (1994).
[30] A. Ponomarenko, D. Quéré, and C. Clanet, J. Fluid Mech. **666**, 146 (2011).
[31] T. Cambau, J. Bico, and E. Reyssat, Europhys. Lett. **96**, 24001 (2011).
[32] X. Shi, M. Brenner, and S. Nagel, Science **265**, 219 (1994).
[33] I. Cohen, M. Brenner, J. Eggers, and S. Nagel, Phys. Rev. Lett. **83**, 1147 (1999).

[34] J. Eggers and E. Villermaux, Rep. Prog. Phys. **71**, 036601 (2008).
[35] J. Savage, M. Caggioni, P. Spicer, and I. Cohen, Soft Matter **6**, 892 (2010).
[36] J. Eggers, J. Lister, and H. Stone, J. Fluid Mech. **401**, 293 (1999).
[37] D. G. A. L. Aarts, H. N. W. Lekkerkerker, H. Guo, G. H. Wegdam, and D. Bonn, Phys. Rev. Lett. **95**, 164503 (2005).
[38] J. C. Burton and P. Taborek, Phys. Rev. Lett. **98**, 224502 (2007).
[39] J. C. Bird, S. Mandre, and H. A. Stone, Phys. Rev. Lett. **100**, 234501 (2008).
[40] S. C. Case and S. R. Nagel, Phys. Rev. Lett. **100**, 084503 (2008).
[41] J. D. Paulsen, J. C. Burton, and S. R. Nagel, Phys. Rev. Lett. **106**, 114501 (2011).
[42] M. Yokota and K. Okumura, Proc. Natl. Acad. Sci. USA **108**, 6395 (2011).
[43] G. Debrégeas, P.-G. de Gennes, and F. Brochard-Wyart, Science **279**, 1704 (1998).
[44] Y. Couder, E. Fort, C.-H. Gautier, and A. Boudaoud, Phys. Rev. Lett. **94**, 177801 (2005).
[45] A. Eri and K. Okumura, Phys. Rev. E **82**, 030601(R) (2010).
[46] A. Eri and K. Okumura, Soft Matter **7**, 5648 (2011).
[47] P.-G. de Gennes, Europhys. Lett. **13**, 709 (1990).
[48] S. Dungan, M. Shapiro, and H. Brenner, Proc. R. Soc. London, Ser. A **429**, 639 (1990).
[49] F. Williams, *Combustion Theory*, 2nd ed. (Benjamin/Cummings, Menlo Park, CA, 1985).